

# Micro-bead injection spectroscopy for label-free automated determination of immunoglobulin G in human serum

Inês I. Ramos<sup>1</sup> · Luís M. Magalhães<sup>1</sup> · Luisa Barreiros<sup>1,2</sup> · Salette Reis<sup>1</sup> · José L. F. C. Lima<sup>3</sup> · Marcela A. Segundo<sup>1</sup>

Received: 10 May 2017 / Revised: 10 July 2017 / Accepted: 23 August 2017 / Published online: 9 September 2017  
© Springer-Verlag GmbH Germany 2017

**Abstract** Immunoglobulin G (IgG) represents the major fraction of antibodies in healthy adult human serum, and deviations from physiological levels are a generic marker of disease corresponding to different pathologies. Therefore, screening methods for IgG evaluation are a valuable aid to diagnostics. The present work proposes a rapid, automatic, and miniaturized method based on UV-vis micro-bead injection spectroscopy ( $\mu$ -BIS) for the real-time determination of human serum IgG with label-free detection. Relying on attachment of IgG in *rec*-protein G immobilized in Sepharose 4B, a bioaffinity column is automatically assembled, where IgG is selectively retained and determined by on-column optical density measurement. A “dilution-and-shoot” approach (50 to 200 times) was implemented without further sample treatment because interferences were flushed out of the column upon sample loading, with minimization of carryover and cross-contamination by automatically discarding the sorbent (0.2 mg) after each determination. No interference from human serum albumin at 60 mg mL<sup>-1</sup> in undiluted sample was found. The method allowed IgG determination in the range

100–300  $\mu$ g mL<sup>-1</sup> (corresponding to 5.0–60 mg mL<sup>-1</sup> in undiluted samples), with a detection limit of 33  $\mu$ g mL<sup>-1</sup> (1.7 mg mL<sup>-1</sup> for samples, dilution factor of 50). RSD values were < 9.4 and < 11.7%, for intra and inter-assay precision, respectively, while recovery values for human serum spiked with IgG at high pathological levels were 97.8–101.4%. Comparison to commercial ELISA kit showed no significant difference for tested samples ( $n = 8$ ). Moreover, time-to-result decreased from several hours to < 5 min and analysis cost decreased 10 times, showing the potential of the proposed approach as a point-of-care method.

**Keywords** Automation · Protein G · Biomarkers · Antibody · Label-free · Biological samples

## Introduction

Immunoglobulins G (IgG) are the major group of antibodies of healthy adult human serum, ranging from 7 to 18 mg mL<sup>-1</sup> [1, 2]. This group of proteins is a valuable serum biomarker for several pathologies that affect directly or have repercussions in the immune system. For instance, decreased levels of IgG may be associated with primary antibody deficiency, protein-losing enteropathies, nephrotic syndrome, or iatrogenic hypogammaglobulinemia as a consequence of immunosuppressant, anti-convulsant, or cytotoxic therapies [3–7]. The level of serum IgG is also a valuable predictor for the risk of infection in transplant recipients [8–10]. Moreover, high IgG levels are indicators of autoimmunity (e.g., demyelinating diseases, lupus erythematosus), chronic infection, liver diseases (e.g., autoimmune hepatitis), and lymphoproliferative disorders (e.g., multiple myeloma) [3, 11–14]. The early diagnosis of these conditions is a key factor to minimize the risk of permanent organ damage and to proceed with adequate therapy, accounting for less morbidity

Published in the topical collection celebrating *ABCs 16th Anniversary*.

✉ Marcela A. Segundo  
mseguno@ff.up.pt

- <sup>1</sup> UCIBIO, REQUIMTE, Department of Chemical Sciences, Faculty of Pharmacy, University of Porto, R Jorge Viterbo Ferreira, 228, 4050-313 Porto, Portugal
- <sup>2</sup> Núcleo de Investigação e Intervenção em Farmácia (NIIF), Centro de Investigação em Saúde e Ambiente (CISA), Escola Superior de Saúde, Instituto Politécnico do Porto, R Dr. António Bernardino de Almeida, 400, 4200-072 Porto, Portugal
- <sup>3</sup> LAQV, REQUIMTE, Department of Chemical Sciences, Faculty of Pharmacy, University of Porto, R Jorge Viterbo Ferreira, 228, 4050-313 Porto, Portugal

and mortality [14, 15]. Metabolic abnormalities (e.g., metabolic syndrome, obesity), smoking, and drinking have also been shown to have a significant impact on IgG levels [1].

The determination of serum IgG level is currently performed by enzyme-linked immunosorbent assay (ELISA), single radial immunodiffusion (SRID), or immuno-nephelometric/turbidimetric methods [16–19]. These batch-wise assays are generally time-consuming and laborious, particularly when it comes to immune recognition schemes because they involve convection-based mass transport of the reagents through the reaction media, requiring long incubation times. In fact, ELISA and SRID are multi-step complex procedures that usually provide large time-to-result intervals (typically up to 6 h for the ELISA and 14–24 h for the SRID assay) [20, 21]. Furthermore, these methods can be highly affected by operational errors and are prone to cross-contamination problems that may occur during washing steps or solution handling, particularly if performed manually. ELISA methods are also highly affected by external conditions, namely temperature, which can impair data validity, known as the “edge effect” [22–24]. Another important aspect is the need of enzyme/antibody conjugates that increase the cost of analysis. As for turbidimetry/nephelometry-based methods, which have been replacing SRID and ELISA in clinical analysis, the main analytical issue is the presence of substances other than antigen-antibody complexes that increase background light scattering or that form precipitates, hampering IgG quantification and affording overestimation [25]. This effect is especially relevant in the presence of high concentrations of protein; thus, sample cleanup steps are often required to minimize interferences.

Recently, label-free approaches have been proposed for the determination of IgG in human serum based on mass spectrometry [26], on magnetically assisted surface enhanced Raman spectroscopy through a  $\text{Fe}_3\text{O}_4@\text{Ag}@\text{streptavidin}@\text{anti-IgG}$  nanocomposite [27], on nanoporous hydrogel photonic crystal structures containing immobilized protein A [28], on attenuated total reflectance mid-infrared spectroscopy coupled to multivariate calibration [29], and on voltammetric detection of IgG binding to reduced graphene oxide@multiwalled carbon nanotube@palladium@anti-IgG nanoparticles [30]. Nevertheless, these methods still require non-portable equipment [26], cumbersome synthesis of materials [28, 30], or advanced data processing [29].

In this context, UV-vis Bead Injection Spectroscopy has been applied to bioanalysis through the combination of flow analysis with on-column optical density measurements to follow bioligand interactions occurring on surfaces [31–35]. In particular, the mesofluidic Lab-on-Valve (LOV) platforms are useful for the miniaturization of bioanalytical assays, namely through micro-Bead Injection Spectroscopy ( $\mu\text{-BIS}$ ) due to their versatility and green chemistry features, as it downscales the consumption of sample and reagents [36].

The applicability of the  $\mu\text{-BIS-LOV}$  strategy for the real-time monitoring of the immobilization of different proteins on

agarose beads was first demonstrated by Ruzicka and co-workers [37], and it has also been used for on-column monitoring of IgG retention in protein G-Sepharose® beads [31]. The use of beads with adequate optical properties allowed the evaluation of binding of IgG from different species (human, rabbit, and horse), but it has not been applied to real samples or to IgG quantification. The field of application of the  $\mu\text{-BIS-LOV}$  strategy was enlarged when Decuir and co-workers [38] performed the capture and simultaneous quantification of biotinylated DNA on solid surfaces. So far, this technique has been employed for the evaluation and optimization of bioaffinity processes, but its potential for clinical applications and point-of-care testing for biomarker assessment remains underexploited. Hence, the aim of this work is the development and application of  $\mu\text{-BIS-LOV}$  for the automated, miniaturized, and direct quantitative determination of IgG in human serum with label-free detection. For this, a molecular recognition strategy will be implemented, using commercially available protein G immobilized in highly cross-linked agarose.

## Experimental

### Chemicals

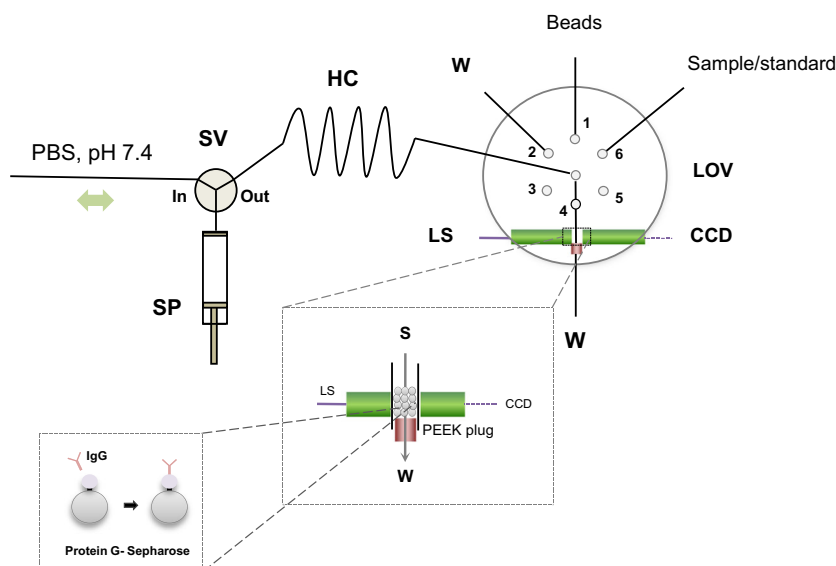
All chemicals used were of analytical reagent grade with no further purification. Water from arium water purification systems (resistivity  $> 18 \text{ M}\Omega \text{ cm}$ , Sartorius, Goettingen, Germany) was used for the preparation of all solutions. Recombinant Protein G-Sepharose® 4B (no. 10-1241) and streptavidin agarose (no. S951) were purchased from Thermo Fisher Scientific (Rockford, IL, USA). Sepharose® CL-4B (no. CL4B200), human IgG standard (no. I2511), and human serum albumin (no. A1887) were obtained from Sigma-Aldrich (St. Louis, MO, USA). HiTrap® Protein A HP columns (no. 17-0403-01) were acquired from GE Healthcare (Chicago, IL, USA). The human IgG ELISA kit (no. RAB0001) used for method validation was also purchased from Sigma-Aldrich.

IgG standard solutions ( $100\text{--}400 \mu\text{g mL}^{-1}$ ) and diluted samples (1:40 to 1:100 times) were prepared in PBS buffer (140 mM NaCl, 16 mM  $\text{Na}_2\text{HPO}_4$ , 2 mM  $\text{KH}_2\text{PO}_4$ , 16 mM EDTA-2Na, pH 7.4). This buffer was also used as carrier solution in the flow system. Prior to use, beads were washed with PBS (pH 7.4) and recovered by centrifugation ( $3326\times g$ , 4 °C, 10 min). These operations were performed four times each.

### $\mu\text{-BIS-LOV}$ configuration and analytical procedure

The LOV equipment (MicroSIA, FIALab Instruments, Inc., Bellevue, WA, USA), depicted in Fig. 1, comprises a 1000- $\mu\text{L}$  bi-directional syringe pump, connected to a two-way valve, a holding coil, and a LOV platform mounted atop

**Fig. 1**  $\mu$ -BIS-LOV configuration for on-column quantification of total human serum IgG. *SP* syringe pump, *SV* solenoid valve connected to the syringe pump, *HC* holding coil, *LS* light source, *CCD* spectrometer, *S* sample/standard, *W* waste. PBS buffer (pH 7.4) was used as carrier



a six-port multi-position valve. It was configured for  $\mu$ -BIS with the following port assignments: (1) beads, (2) waste, (4) flow cell, and (6) sample/standard. Ports 3 and 5 were not used. The flow cell (optical path 1.6 mm) was illuminated by a 600- $\mu$ m fiber-optic cable connected to the light source (deuterium-halogen light source model DH-2000, Top Sensor Systems, Eerbeek, The Netherlands). Emerging radiation was collected by another 600  $\mu$ m fiber optic cable, connected to a USB4000-UV-vis CCD spectrometer (Ocean Optics, El Dorado Hills, CA, USA). A PEEK plug (0.13 mm ID, 3 mm

long) was placed immediately below the light beam to retain the beads inside the flow cell, allowing the liquid to flow out. The system was operated at room temperature, controlled by a personal computer running FIAlab software (FIAlab Instruments, Inc.), version 5.9.320.

The analytical cycle for bead column assembly and IgG determination is detailed in Table 1. For each determination, analysis started by packing a fresh immunoaffinity column inside the flow cell (Table 1, routine A). The bead suspension placed in port 1 was dispersed by flushing 4  $\mu$ L of PBS into this port followed

**Table 1**  $\mu$ -BIS-LOV analytical cycles for the determination of total human IgG

Step	LOV valve position	Flow rate ( $\mu\text{L s}^{-1}$ )	Volume ( $\mu\text{L}$ )	SP valve position <sup>a</sup>	Description
Routine A: packing of bead column (30 s)					
I	2	200	600	In	Aspirate carrier into syringe
II	1	3	4	Out	Flush and disperse solid phase
III	1	5	10	Out	Aspirate beads into central channel
IV	4	5	8	Out	Send beads to the flow cell
V	2	200	400	Out	Discard excess of beads to waste
VI	4	10	194	Out	Conditioning of bead column
Routine B: IgG quantification (131 s)					
VII	2	200	800	In	Aspirate carrier into syringe
VIII	4	1	20	Out	Acquire reference scan
IX	6	3	20	Out	Aspirate sample into HC
X	4	1	100	Out	Signal acquisition while sending HC content to the flow cell
Routine C: removal of bead column (28 s)					
XI	4	100	200	Out	Aspirate column beads into the central channel
XII	–	100	800	In	Aspirate carrier into syringe
XIII	2	200	1000	Out	Discard beads
XIV	–	100	1000	In	Aspirate carrier into syringe
XV	4	400	1000	Out	Wash flow cell

<sup>a</sup>“Valve Out” position connects the syringe pump (SP) to the LOV central channel. “Valve In” position means that the syringe pump is connected to the carrier reservoir

by immediate aspiration of 10  $\mu\text{L}$  of the suspension, at a low flow rate (3–5  $\mu\text{L s}^{-1}$ ). Eight microliters of the bead suspension was then sent to the flow cell and conditioned with 194  $\mu\text{L}$  of PBS at 10  $\mu\text{L s}^{-1}$ . During *routine B* (Table 1), aiming at IgG assessment, 20  $\mu\text{L}$  of standard or sample previously diluted in carrier was aspirated and flushed through the beads' column at a low flow rate (1  $\mu\text{L s}^{-1}$ ) to allow IgG interaction with protein G. The interaction/immobilization process is monitored by measuring the optical density at 280 nm elicited through the solid support, that is the attenuation of light intensity caused both by absorbance and light scattering of IgG present in samples. By the end of each complete analytical cycle, the bead column was discarded by back-aspiration at a high flow rate (100  $\mu\text{L s}^{-1}$ ) and the flow cell was washed (Table 1, *routine C*) and prepared for the packing of a new column.

### Method validation by microplate ELISA

For comparison purposes, the concentration of IgG in the serum of eight healthy individuals was assessed by the developed  $\mu\text{-BIS-LOV}$  method and by the commercially available microplate ELISA kit. This assay is based on human IgG antibody-coated plate and detection by biotinylated human IgG, horseradish peroxidase-streptavidin conjugate, and 3,3',5,5'-tetramethylbenzidine as colorimetric substrate. Sample preparation and ELISA procedures for total human IgG detection were carried out according to manufacturer's instructions. Absorbance at 450 nm was measured using a Cytation3® microplate reader (BioTek instruments, Winoosky, VT, USA) operated by Gen5 software. Paired *t* test was applied to compare the results obtained using both methods.

## Results and discussion

### Development of $\mu\text{-BIS-LOV}$ method

The  $\mu\text{-BIS-LOV}$  method for the determination of serum IgG consisted on a bioaffinity separative approach using a solid phase containing an active bioligand. Method development was directed towards the establishment of a straightforward procedure without any incubation periods or stopped-flow steps in order to attain a high-throughput procedure. Additionally,  $\mu\text{-BIS-LOV}$  allows the analyte to be actively flushed through the solid phase, so it does not rely on convection-based diffusion. Hence, IgG deposition on the solid phase was evaluated by direct, on-column UV-vis spectroscopy (280 nm), as schematically depicted in Fig. 1.

It was possible to apply a continuous flow strategy for sample injection setting the flow rate to the minimum achievable by the LOV equipment with a 1-mL syringe (1  $\mu\text{L s}^{-1}$ ). Higher flow rates decreased the contact time between IgG and the bioaffinity elements embedded in the bead column and,

thus, retention was lower (data not shown). Initially, two ligands (protein A and protein G) and three supports (Sepharose CL-4B, Sepharose CL-6B, and streptavidin 4B Sepharose) were evaluated. It was observed that the nature of the retaining proteins embedded in the agarose column affected the stability of the acquired signal during flow conditions. For instance, Sepharose 4B containing either protein A or protein G presented different baseline profiles when 20  $\mu\text{L}$  of buffer was injected at 1  $\mu\text{L s}^{-1}$ , as shown in Fig. 2. The same experiment was performed for protein A bound to Sepharose by a streptavidin bridge. For all conditions tested with protein A, light scattering was high (> 0.100 within 300 s) and did not allow to detect IgG deposition at 400  $\mu\text{g mL}^{-1}$ . Protein G beads provided low light scattering and lower baseline variation (< 0.030 within 300 s), allowing repeatable on-column monitoring of IgG attachment to bead surface.

Additionally, protein G is more specific to IgG capture than protein A, which also binds to human IgM, IgD, and IgA with lower affinity. Hence, serum matrix components (including immunoglobulins belonging to other classes) are not retained in the protein G column, being immediately flushed to waste. Finally, human IgG also bind to protein G (association constant between  $10^7$  and  $10^{10} \text{ M}^{-1}$ ) with greater affinity than protein A [39, 40]. Therefore, protein G-Sepharose 4B was chosen as solid support. Diameter distribution of those microbeads ranges from 45 to 165  $\mu\text{m}$ , provided that the matrix comprises Sepharose with 4% of cross-linking. The beads present micro-pores in their structure, which set the molecular weight cutoff between  $6 \times 10^4$  and  $2 \times 10^7$  for globular proteins. Regarding binding features, the solid support contains 2.5 mg of protein G per mL with 2 IgG binding sites per molecule. Binding affinity was ca. 18 mg of IgG per mL of solid support.

The study of the bead column packing LOV procedure (Table 1, *routine A*) was carried out using non-functionalized Sepharose CL-4B. To ensure the repeatability of the bead aspiration and packing inside the flow cell, beads were first flushed

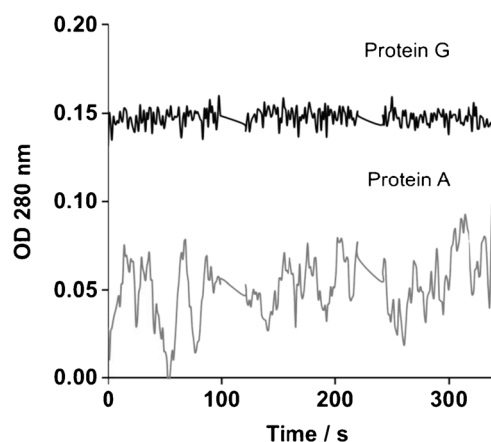
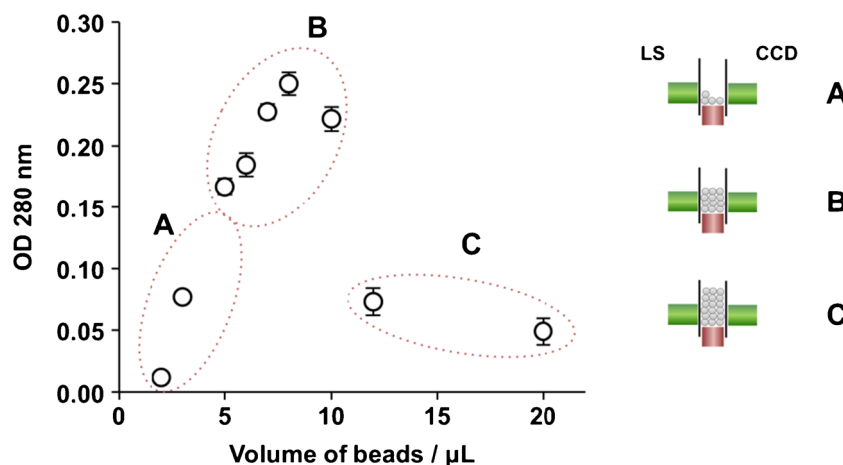


**Fig. 2** Baseline profile for Sepharose 4B beads with immobilized protein G or immobilized protein A (*flow rate*, 1  $\mu\text{L s}^{-1}$ )

**Fig. 3** Optical density (OD 280 nm) corresponding to loading 20  $\mu\text{L}$  of human IgG ( $300 \mu\text{g mL}^{-1}$ ) in protein G bioaffinity columns packed from different volumes of bead suspension. Schematic representation of column assembly at flow cell upon bead suspension volume. *LS* light source, *CCD* spectrometer



and dispersed inside the storage port 1 (Table 1, step II) and then back aspirated into the holding coil [41] (Table 1, step III). Several flushing flow rates ( $1\text{--}10 \mu\text{L s}^{-1}$ ) and volumes ( $1\text{--}10 \mu\text{L}$ ) were tested. Bead dispersion inside the channel of port 1 was achieved by sending  $4 \mu\text{L}$  at  $3 \mu\text{L s}^{-1}$ . Aspiration flow rate for bead transfer into the holding coil was set to  $5 \mu\text{L s}^{-1}$  to avoid the introduction of air bubbles in the system.

Subsequently, experiments to establish the volume of bead suspension aspirated from port 1 (Table 1, step IV) and sent for column assembly were carried out, using volumes between 2 and 20  $\mu\text{L}$ . This is an important parameter to evaluate because the amount of beads sent to the flow cell to pack the column affects method sensitivity as it will determine the position of the solid phase with respect to the light beam (Fig. 3, schematic representation). Hence, after packing the column, a solution containing  $300 \mu\text{g mL}^{-1}$  of human IgG was propelled through the column at  $1 \mu\text{L s}^{-1}$  and optical density (OD 280 nm) values were plotted against volume of beads sent to the flow cell (Fig. 3) as signal intensity reflects the amount of IgG that gets retained within the optical path [42]. Bead suspension volumes  $< 5 \mu\text{L}$  did not provide enough material for sensitive IgG retention (Fig. 3, zone A in the graph) and thus OD values were  $< 0.100$ . For volumes between 5 and 10  $\mu\text{L}$  (Fig. 3, zone B in the graph), small variations on the amount of beads sent into the flow cell afforded differences on signal intensity. The highest OD values were obtained for 8  $\mu\text{L}$  ( $0.250 \pm 0.009$ ). At this volume, the beads occupied the entire optical path as checked visually and schematically depicted in Fig. 3, scheme B. Larger volumes (10 to 20  $\mu\text{L}$ ) led to lower OD values ( $< 0.070$ ) because IgG was mainly retained in the top part of the bead column, decreasing the amount of IgG in the solid phase exposed to the light beam (Fig. 3, scheme C). Therefore, bead volume was set to 8  $\mu\text{L}$  in order to maximize signal intensity. Moreover, under these conditions, baseline noise is negligible ( $\Delta OD_{280} < 0.0003 \text{ s}^{-1}$ ) and ca. 200  $\mu\text{g}$  of solid support is required per analysis.

Sample volume was also tested by injecting 5, 10, 20, and 40  $\mu\text{L}$  of IgG at  $300 \mu\text{g mL}^{-1}$ . Recovered mass was 1.6, 2.8, 5.9,

and 10.9  $\mu\text{g}$ , representing relative deviations  $< 6.5\%$  from the theoretical value, except for the largest volume. In this case, IgG mass surpassed the established linear range for response. These features (including label-free, on-column detection) allow the operator to perform the evaluation of IgG content in real-time by assaying different sample volumes, avoiding unnecessary runs with a consequent reduction in reagents consumption and generation of waste. In opposition, when samples are analyzed by microplate ELISA, it is also mandatory to prepare and run several dilutions of the sample in parallel to overcome matrix

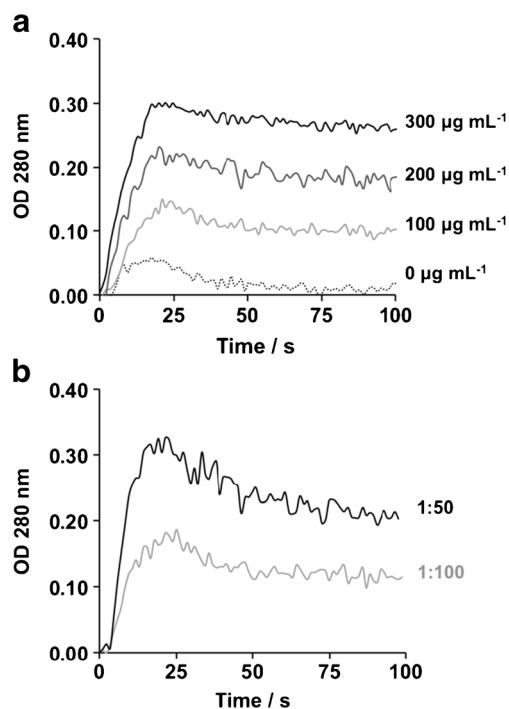


**Fig. 4**  $\mu\text{-BIS}$  signal of **a** IgG standard solutions (concentration of standards in  $\mu\text{g mL}^{-1}$ , corresponding to 5.0–60  $\text{mg mL}^{-1}$  in undiluted samples), prepared in PBS +  $1.0 \mu\text{g mL}^{-1}$  of human serum albumin. **b** Human serum samples diluted in PBS at two levels (1:50 and 1:100). Injection volume was 20  $\mu\text{L}$

effect and non-specific binding. Hence, this is a clear advantage of the automated  $\mu$ -BIS-LOV method.

### Figures of merit of $\mu$ -BIS-LOV IgG assay

Typical analytical signals obtained for IgG standard solutions are shown in Fig. 4a, where the time-point 0 s corresponds to the sample injection point. Signal stabilization is achieved after 75 s and the average value of OD obtained between 82 and 92 s was considered for establishing a relation between the OD 280 nm and IgG concentration in  $\mu\text{g mL}^{-1}$ . Calibration curves were established between 100 and 300  $\mu\text{g mL}^{-1}$ , with a typical equation of  $y = 0.749 \pm 0.023x + 0.021 \pm 0.016$ ,  $R > 0.9975$ . For concentrations above 300  $\mu\text{g mL}^{-1}$ , signal increase was observed but its relation to concentration was not linear.

The limit of detection (LOD) was calculated as the concentration corresponding to the intercept value of the calibration curve plus three times the statistics  $s_{y/x}$  as an estimate of the standard deviation [43]. Hence, LOD was 33  $\mu\text{g mL}^{-1}$ , corresponding to 1.7  $\text{mg mL}^{-1}$  in samples diluted 50 times (lowest dilution factor).

The overall time of analysis was estimated by adding the time taken by each step of the protocol routines (Table 1). Routines A, B, and C took 30, 131, and 28 s, respectively. Sample exchange operation (ca. 60 s) was also considered. Therefore, the time required for a complete analytical cycle was 4.1 min, setting the determination rate at 15  $\text{h}^{-1}$ . Therefore, compared to ELISA procedures, time to result was reduced from several hours to < 5 min.

Precision was estimated for both the lowest (100  $\mu\text{g mL}^{-1}$ ) and the highest (300  $\mu\text{g mL}^{-1}$ ) levels of the calibration curve. Concerning intra-assay precision, four consecutive injections were carried out affording RSD values < 9.4% (100  $\mu\text{g mL}^{-1}$ ) and < 5.0% (300  $\mu\text{g mL}^{-1}$ ). As for inter-assay precision ( $n = 3$ ), RSD values found were < 11.7 and < 8.8% for the lowest and the highest levels, respectively.

The developed method provided a miniaturized label-free assay with no need for the use of secondary antibodies, enzyme conjugates, or revealing agents and, for that reason, the cost of the overall analysis was decreased around 10 times when compared to the microplate ELISA. The estimate cost per analysis is ca. 0.60 € for the  $\mu$ -BIS-LOV and ca. 6 € for the commercial microplate ELISA kit.

### Analysis of serum samples

Sample preparation consisted on a “dilute-and-shoot” procedure. Before analysis, samples were diluted 50 to 200 times to match the linear range of the calibration curve and also to circumvent possible matrix effects caused by other serum proteins, providing a determination range of 5.0–60  $\text{mg mL}^{-1}$ . Twenty microliters of diluted sample was required for each determination. Therefore, the undiluted sample volume

required for analysis was very low (1–6  $\mu\text{L}$  per analysis). In addition, sample dilution also afforded control of reaction pH and ionic strength, which is critical to IgG adsorption/desorption to protein G.

Human serum albumin (HSA) is the most abundant protein in serum and, thus, it was chosen as a model protein to assess the possible interference in the  $\mu$ -BIS measurements. In physiological conditions, HSA is present in human serum at concentrations between 35 and 55  $\text{mg mL}^{-1}$  [44–46]. After the proposed sample dilution (at least 50 times), the average HSA concentration would be < 1.1  $\text{mg mL}^{-1}$ . Hence, HSA presence up to 1.2  $\text{mg mL}^{-1}$  was evaluated. The signal variation obtained for a solution containing 250  $\mu\text{g mL}^{-1}$  of IgG was recorded in the presence of increasing concentrations of HSA (0.7–1.2  $\text{mg mL}^{-1}$ ) and compared to the one obtained when no HSA was present. Comparing the maximum OD values obtained when the IgG standard is prepared in PBS and in PBS-HSA, it was observed that the deviation of OD values was < 5.5%. Furthermore, calculated IgG concentrations were 99.0–107% of the target value. Thus, matrix effect was not significant for HSA concentrations < 1.2  $\text{mg mL}^{-1}$ , accounting up to 60  $\text{mg mL}^{-1}$  in undiluted serum.

To confirm the absence of matrix effects, recovery tests were performed using spiked human serum containing 10.6  $\text{mg mL}^{-1}$  of IgG. Two spiking levels were considered to simulate two different stages of multiple myeloma development: monoclonal gammopathy of undetermined significance or MGUS ( $[\text{IgG}] < 30 \text{ mg mL}^{-1}$ ) and asymptomatic myeloma ( $[\text{IgG}] > 30 \text{ mg mL}^{-1}$ ). Thus, serum was spiked to a final concentration of 17.8 and 40.5  $\text{mg mL}^{-1}$  in IgG. Recovery values were  $101.4 \pm 3.4$  and  $97.8 \pm 3.0\%$ , respectively, using dilution factors at two levels (100 to 200 times).

The IgG concentration in the serum of eight individuals (serum A to H) was determined by  $\mu$ -BIS-LOV and microplate ELISA kit (Table 2). The typical analytical profiles obtained for serum samples at two levels of dilution (1:50 and

**Table 2** IgG concentration ( $\text{mg mL}^{-1}$ ) in human serum samples (mean  $\pm$  standard deviation) obtained by  $\mu$ -BIS-LOV ( $C_{\mu\text{-BIS-LOV}}$ ) and the microplate ELISA kit ( $C_{\text{ELISA}}$ )

Sample <sup>a</sup>	$C_{\mu\text{-BIS-LOV}}$	$C_{\text{ELISA}}$
Serum A	12.0 $\pm$ 0.9	13.0 $\pm$ 0.1
Serum B	14.1 $\pm$ 1.0	13.8 $\pm$ 0.1
Serum C	13.2 $\pm$ 0.6	12.9 $\pm$ 0.7
Serum D	10.4 $\pm$ 1.0	10.2 $\pm$ 0.6
Serum E	6.7 $\pm$ 0.1	5.5 $\pm$ 0.7
Serum F	11.6 $\pm$ 1.2	11.9 $\pm$ 0.5
Serum G	13.8 $\pm$ 0.9	13.2 $\pm$ 0.9
Serum H	14.1 $\pm$ 1.3	14.8 $\pm$ 0.8

<sup>a</sup> Each value corresponds to the mean  $\pm$  standard deviation ( $n = 2$ ). Prior to analysis by  $\mu$ -BIS-LOV assay and ELISA, samples were diluted 50 to 100 times and 10<sup>6</sup> times, respectively

1:100) are provided in Fig. 4b. The results obtained for the developed label-free method were in good agreement with those obtained using the ELISA commercial kit. Paired *t* test was performed and the  $|t|_{\text{calculated}}$  value was 0.055 ( $t_{\text{tabulated}} (P = 0.05; df = 14) = 2.14$ ). Hence, no statistically significant difference was found for results obtained by the two methods. Repeatability for sample analysis was also evaluated. The overall precision (RSD 1.5–10.3%) was comparable to the microplate ELISA kit (RSD 0.7–12.7%). Additionally, three samples selected randomly (A, F, and G) were diluted at 1:100 and run in triplicate providing RSD values of 1.9, 8.0, and 10.2%, respectively. Serum sample C was also diluted at 1:100 and injected five consecutive times with RSD value < 9.0%.

## Conclusions

The  $\mu$ -BIS-LOV method allows real-time on-column and label-free determination of total serum IgG under a miniaturized format. Immunoglobulins are separated from the serum matrix components, followed by their quantification, avoiding matrix interferences and non-specific binding. The proposed method provides a rapid, automated, and label-free determination of these biomarkers with a consequent decrease in the cost of the analysis, compared to the standard ELISA method. In addition, no sample pretreatment was required besides dilution and reaction conditions were strictly controlled by automatic handling of solutions, ensuring good repeatability of the measurements within a short time. Washing steps were not required because the excess of unbound antibodies and other proteins was automatically flushed away upon sample percolation through the bead column. Issues concerning sample carryover and fouling of the solid support were fully eliminated by discarding and assembling of a new column before each sample determination. Analytical features proved the method fit for purpose.

Due to the portability of the equipment and the simplicity of the procedure, we envision that the proposed method is suitable for point-of-care testing, overcoming the need for sample analysis in hospital facilities and providing a fast analytical readout. Therefore, the developed method provides a suitable cost-effective and fast alternative for the direct measurement of IgG in serum.

**Acknowledgements** I.I. Ramos and L. Barreiros thank Fundação para a Ciência e a Tecnologia (FCT) and Programa Operacional Potencial Humano (POPH) for their grants (SFRH/BD/97540/2013 and SFRH/BPD/89668/2012).

**Funding Information** The authors also acknowledge financial support from The European Union (FEDER funds POCI/01/0145/FEDER/007728 and POCI/01/0145/FEDER/007265) and National Funds (FCT/MEC, Fundação para a Ciência e a Tecnologia and Ministério da

Educação e Ciência) under the Partnership Agreements PT2020 UID/MULTI/04378/2013 and PT2020 UID/QUI/50006/2013.

**Compliance with ethical standards** Authentic human serum samples were collected and analyzed anonymously from nine different healthy volunteers who provided written informed consent. According to Portuguese legislation, the aim of this research is not within the scope of clinical investigation.

**Conflict of interest** The authors declare that they have no conflict of interest.

## References

- Gonzalez-Quintela A, Alende R, Gude F, Campos J, Rey J, Meijide LM, et al. Serum levels of immunoglobulins (IgG, IgA, IgM) in a general adult population and their relationship with alcohol consumption, smoking and common metabolic abnormalities. *Clin Exp Immunol.* 2008;151(1):42–50.
- Ritchie RF, Palomaki GE, Neveux LM, Navolotskaia O. Reference distributions for immunoglobulins A, G, and M: a comparison of a large cohort to the world's literature. *J Clin Lab Anal.* 1998;12(6): 371–7.
- Holding S, Jolles S. Current screening approaches for antibody deficiency. *Curr Opin Allergy Clin Immunol.* 2015;15(6):547–55.
- Duraisingham SS, Buckland M, Dempster J, Lorenzo L, Grigoriadou S, Longhurst HJ. Primary vs. secondary antibody deficiency: clinical features and infection outcomes of immunoglobulin replacement. *PLoS One.* 2014;9(6):e100324.
- Duraisingham SS, Buckland MS, Grigoriadou S, Longhurst HJ. Secondary antibody deficiency. *Expert Rev Clin Immunol.* 2014;10(5):583–91.
- Furst DE. Serum immunoglobulins and risk of infection: how low can you go? *Semin Arthritis Rheum.* 2009;39(1):18–29.
- van der Burg M, van Zelm MC, Driessen GJA, van Dongen JJM. New frontiers of primary antibody deficiencies. *Cell Mol Life Sci.* 2012;69(1):59–73.
- Sarmiento E, Rodriguez-Molina JJ, Fernandez-Yañez J, Palomo J, Urrea R, Muñoz P, et al. IgG monitoring to identify the risk for development of infection in heart transplant recipients. *Transpl Infect Dis.* 2006;8(1):49–53.
- Fernandez-Ruiz M, Lopez-Medrano F, Varela-Pena P, Lora-Pablos D, Garcia-Reyne A, Gonzalez E, et al. Monitoring of immunoglobulin levels identifies kidney transplant recipients at high risk of infection. *Am J Transplant.* 2012;12(10):2763–73.
- Doron S, Ruthazer R, Werner BG, Rabson A, Snyderman DR. Hypogammaglobulinemia in liver transplant recipients: incidence, timing, risk factors, and outcomes. *Transplantation.* 2006;81(5): 697–703.
- Fallatah HI, Akbar HO. Elevated serum immunoglobulin G levels in patients with chronic liver disease in comparison to patients with autoimmune hepatitis. *Libyan J Med.* 2010;5:4857.
- Kyle RA, Durie BGM, Rajkumar SV, Landgren O, Blade J, Merlini G, et al. Monoclonal gammopathy of undetermined significance (MGUS) and smoldering (asymptomatic) multiple myeloma: IMWG consensus perspectives risk factors for progression and guidelines for monitoring and management. *Leukemia.* 2010;24(6):1121–7.
- Lim DH, Kim YG, Lee D, Ahn SM, Hong S, Lee CK, et al. Immunoglobulin G levels as a prognostic factor for autoimmune hepatitis combined with systemic lupus erythematosus. *Arthritis Care Res.* 2016;68(7):995–1002.

14. Compagno N, Malipiero G, Cinetto F, Agostini C. Immunoglobulin replacement therapy in secondary hypogammaglobulinemia. *Front Immunol.* 2014;5:1–6.
15. Bright PD, Rooney N, Virgo PF, Lock RJ, Johnston SL, Unsworth DJ. Laboratory clues to immunodeficiency; missed chances for early diagnosis? *J Clin Pathol.* 2015;68(1):1–5.
16. Etzel LR, Strohbahn RE, McVicker JK. Development of an automated turbidimetric immunoassay for quantification of bovine serum immunoglobulin G. *Am J Vet Res.* 1997;58(11):1201–5.
17. Blanchard GC, Gardner R. Two nephelometric methods compared with a radial immunodiffusion method for the measurement of IgG. IgA and IgM *Clin Biochem.* 1980;13(2):84–91.
18. Alexander RL. Comparison of radial immunodiffusion and laser nephelometry for quantitating some serum proteins. *Clin Chem.* 1980;26(2):314–7.
19. Engvall E, Perlmann P. Enzyme-linked immunosorbent assay (ELISA) quantitative assay of immunoglobulin G. *Immunochemistry.* 1971;8(9):871–4.
20. Mancini G, Carbonara AO, Heremans JF. Immunochemical quantitation of antigens by single radial immunodiffusion. *Immunochemistry.* 1965;2(3):235–IN6.
21. Gelsing SL, Smith AM, Jones CM, Heinrichs AJ. Technical note: comparison of radial immunodiffusion and ELISA for quantification of bovine immunoglobulin G in colostrum and plasma. *J Dairy Sci.* 2015;98(6):4084–9.
22. Grandke J, Resch-Genger U, Bremser W, Garbe L-A, Schneider RJ. Quality assurance in immunoassay performance-temperature effects. *Anal Methods.* 2012;4(4):901–5.
23. Roselle C, Verch T, Shank-Retzlaff M. Mitigation of microtiter plate positioning effects using a block randomization scheme. *Anal Bioanal Chem.* 2016;408(15):3969–79.
24. Grandke J, Oberleitner L, Resch-Genger U, Garbe LA, Schneider RJ. Quality assurance in immunoassay performance—comparison of different enzyme immunoassays for the determination of caffeine in consumer products. *Anal Bioanal Chem.* 2013;405(5):1601–11.
25. Agarwal S, Cunningham-Rundles C. Assessment and clinical interpretation of reduced IgG values. *Ann Allergy Asthma Immunol.* 2007;99(3):281–3.
26. Hong QT, Lebrilla CB, Miyamoto S, Ruhaak LR. Absolute quantitation of immunoglobulin G and its glycoforms using multiple reaction monitoring. *Anal Chem.* 2013;85(18):8585–93.
27. Balzerova A, Fargasova A, Markova Z, Ranc V, Zboril R. Magnetically-assisted surface enhanced Raman spectroscopy (MA-SERS) for label-free determination of human immunoglobulin G (IgG) in blood using Fe<sub>3</sub>O<sub>4</sub>@Ag nanocomposite. *Anal Chem.* 2014;86(22):11107–14.
28. Choi E, Choi Y, Nejad YHP, Shin K, Park J. Label-free specific detection of immunoglobulin G antibody using nanoporous hydrogel photonic crystals. *Sens Actuator B-Chem.* 2013;180:107–13.
29. Hou S, Riley CB, Mitchell CA, Shaw RA, Bryanton J, Bigsby K, et al. Exploration of attenuated total reflectance mid-infrared spectroscopy and multivariate calibration to measure immunoglobulin G in human sera. *Talanta.* 2015;142:110–9.
30. Liu L, Li YY, Tian LH, Guo T, Cao W, Wei Q. A label-free voltammetric immunoassay based on 3D-structured rGO-MWCNT-Pd for detection of human immunoglobulin G. *Sens Actuator B-Chem.* 2015;211:170–6.
31. Gutzman Y, Carroll AD, Ruzicka J. Bead injection for biomolecular assays: affinity chromatography enhanced by bead injection spectroscopy. *Analyst.* 2006;131(7):809–15.
32. Carroll AD, Scampavia L, Ruzicka J. Label dilution method: a novel tool for bioligand interaction studies using bead injection in the lab-on-valve format. *Analyst.* 2002;127(9):1228–32.
33. Ogata Y, Scampavia L, Ruzicka J, Scott CR, Gelb MH, Tureček F. Automated affinity capture–release of biotin-containing conjugates using a lab-on-valve apparatus coupled to UV/visible and electrospray ionization mass spectrometry. *Anal Chem.* 2002;74(18):4702–8.
34. Carroll AD, Scampavia L, Luo D, Lernmark A, Ruzicka J. Bead injection ELISA for the determination of antibodies implicated in type 1 diabetes mellitus. *Analyst.* 2003;128(9):1157–62.
35. Ruzicka J, Ivaska A. Bioligand interaction assay by flow injection absorptiometry. *Anal Chem.* 1997;69(24):5024–30.
36. Hansen EH, Miro M. Interfacing microfluidic handling with spectroscopic detection for real-life applications via the lab-on-valve platform: a review. *Appl Spectrosc Rev.* 2008;43(4):335–57.
37. Ruzicka J, Carroll AD, Lahdesmaki I. Immobilization of proteins on agarose beads, monitored in real time by bead injection spectroscopy. *Analyst.* 2006;131(7):799–808.
38. Decuir M, Lahdesmaki I, Carroll AD, Ruzicka J. Automated capture and on-column detection of biotinylated DNA on a disposable solid support. *Analyst.* 2007;132(8):818–22.
39. Saha K, Bender F, Gizeli E. Comparative study of IgG binding to proteins G and A: nonequilibrium kinetic and binding constant determination with the acoustic waveguide device. *Anal Chem.* 2003;75(4):835–42.
40. Akerstrom B, Bjorck L. A physicochemical study of protein G, a molecule with unique immunoglobulin G-binding properties. *J Biol Chem.* 1986;261(22):10240–7.
41. Oliveira HM, Miro M, Segundo MA, Lima JLFC. Universal approach for mesofluidic handling of bead suspensions in lab-on-valve format. *Talanta.* 2011;84(3):846–52.
42. Miro M, Frenzel W, Cerda V, Estela JM. Determination of ultratrace nitrite by solid-phase preconcentration using a novel flow-through spectrophotometric optrode. *Anal Chim Acta.* 2001;437(1):55–65.
43. Miller JN, Miller JC. *Statistics and chemometrics for analytical chemistry.* 5th ed. Essex: Pearson Education; 2005.
44. Hosafci G, Klein O, Oremek G, Mantele W. Clinical chemistry without reagents? An infrared spectroscopic technique for determination of clinically relevant constituents of body fluids. *Anal Bioanal Chem.* 2007;387(5):1815–22.
45. Doweiko JP, Nompoggi DJ. The role of albumin in human physiology and pathophysiology .3. Albumin and disease states. *J Parenter Enter Nutr.* 1991;15(4):476–83.
46. Cirelli N, Lebrun P, Gueuning C, Delogne-Desnoeck J, Vanbellinghen AM, Graff G, et al. Physiological concentrations of albumin stimulate chorionic gonadotrophin and placental lactogen release from human term placental explants. *Hum Reprod.* 2001;16(3):441–8.